

NNLO QCD corrections to the Higgs-strahlung processes at hadron colliders

OLIVER BREIN¹, ABDELHAK DJOUADI^{2,3} and ROBERT HARLANDER²

¹ Max-Planck-Institut für Physik, Föhringer Ring 6, D–80805 Munich, Germany.

² Theory Division, CERN, CH–1211 Geneva 23, Switzerland.

³ Laboratoire de Physique Mathématique et Théorique, UMR5825–CNRS,
Université de Montpellier II, F–34095 Montpellier Cedex 5, France.

Abstract

We implement, at next-to-next-to-leading order, the QCD corrections to Standard Model Higgs boson production in association with vector bosons at hadron colliders, $q\bar{q} \rightarrow HV$ with $V = W, Z$. They consist of the two-loop corrections to the Drell–Yan process for the production of off-shell vector bosons, $q\bar{q} \rightarrow V^*$, and in the case of Z final states, of the additional contribution from heavy-quark loop mediated processes, in particular $gg \rightarrow HZ$. For the Higgs boson masses relevant at the Tevatron and the LHC, $M_H \lesssim 200\text{--}300$ GeV, the two-loop corrections are small, increasing the production cross sections by less than 5% and 10%, respectively; the scale dependence is reduced to a level of less than a few per cent. This places these processes among the most theoretically clean Higgs boson production channels at hadron colliders.

1. Introduction

The Standard Model (SM) predicts the existence of a scalar particle, the Higgs boson, that is the remnant of the electroweak symmetry-breaking mechanism that generates the weak gauge boson and fermion masses [1]. The search for this particle is the primary mission of present and future high-energy colliders. The Higgs boson can be discovered at Run II of the Tevatron if it is relatively light, $M_H \lesssim 200$ GeV, as suggested by the fits to the high-precision electroweak data [2], and if sufficient integrated luminosity is collected [3, 4]. Higgs bosons with masses up to $M_H \sim 1$ TeV, a value beyond which perturbation theory is jeopardized in the SM, can be probed at the upcoming LHC [5, 4].

One of the most important Higgs boson production mechanisms at hadron colliders is the Higgs-strahlung process, i.e. the associated production of Higgs and weak gauge bosons, $q\bar{q} \rightarrow HV$ with $V = W, Z$ [6]. At the Tevatron, Higgs particles can be mainly produced in the channel $q\bar{q} \rightarrow HW$ with the W boson decaying into $\ell\nu$ pairs [with $\ell = e, \mu$] and the Higgs boson decaying into $b\bar{b}$ or W^+W^- pairs [7]. At the LHC, a plethora of production channels can be used to search for the Higgs particle; one of the principal detection modes is expected to be the gluon-gluon fusion process, $gg \rightarrow H$ [8, 9], with the signatures $H \rightarrow \gamma\gamma$ or $H \rightarrow ZZ^{(*)}, WW \rightarrow 4\ell$ in, respectively, the low and high Higgs mass ranges. However, although with more difficulty, the Higgs boson can also be detected through the channels $q\bar{q} \rightarrow HW/HZ$, in particular in the $\gamma\gamma$ plus lepton final states [10, 11]. These processes could play a very important role in the determination of the Higgs boson properties [12].

It is well known that, in hadronic collisions, the lowest-order (LO) cross sections are affected by large uncertainties arising from higher-order QCD corrections. If at least the next-to-leading order (NLO) radiative corrections are included, the cross sections can be defined properly and their unphysical variation with the scales are stabilized. To have an even better control on the theoretical prediction, the next-to-next-to-leading order (NNLO) corrections, which are in general very complicated to calculate, are desirable. Up to now, the NNLO corrections to SM Higgs boson production at hadron colliders are known only for the $gg \rightarrow H$ mechanism [9] in the infinite top quark mass limit¹.

In this paper, we will discuss the NNLO order, i.e. the $\mathcal{O}(\alpha_s^2)$, corrections to the $pp \rightarrow HV$ production cross sections [hereafter, we will use the notation pp for both pp and $p\bar{p}$]. Part of these corrections are simply those of the Drell-Yan process $pp \rightarrow V$; however, in the case of $pp \rightarrow HZ$, additional corrections are due to diagrams involving the Zgg vertex as well as to loop-induced gg fusion diagrams. We show that while the NNLO corrections increase the cross sections by only 5 to 10%, the scale dependence of the latter is drastically reduced, making these channels among the theoretically cleanest Higgs production mechanisms.

¹The NNLO corrections to the bottom-quark fusion mechanism, $b\bar{b} \rightarrow H + X$, which plays an important role in supersymmetric extensions of the SM, have also been derived recently [13].

The paper is organized as follows. In the next section, we describe the known behaviour of the production cross section at leading and next-to-leading orders in QCD. In section 3, we summarize the main contributions to the cross section at NNLO: the Drell–Yan corrections and the additional corrections to HZ production due to gluon–gluon-initiated processes. The numerical results for the K -factors, the variation with the renormalization and factorization scales are summarized in section 4. A short conclusion and some remarks on the remaining uncertainties on the production cross section are given in the last section.

2. LO and NLO cross sections

The associated production of Higgs and gauge bosons, Fig. 1, is one of the simplest production mechanisms at hadron colliders: the final state does not feel strong interactions, which affect only the quark and antiquark initial state. In fact, this process can be viewed simply as the Drell–Yan production of a virtual W or Z boson, which then splits into a real vector boson and a Higgs particle. Denoting by k the momentum of the virtual gauge boson, the energy distribution of the full subprocess can be written at leading order as

$$\frac{d\hat{\sigma}}{dk^2}(q\bar{q} \rightarrow HV) = \sigma(q\bar{q} \rightarrow V^*) \times \frac{d\Gamma}{dk^2}(V^* \rightarrow HV) , \quad (1)$$

where, in terms of $0 \leq k^2 \leq Q^2 = \hat{s}$ with \hat{s} the centre-of-mass energy of the subprocess and the usual two-body phase-space function $\lambda(x, y; z) = (1 - x/z - y/z)^2 - 4xy/z^2$, one has

$$\frac{d\Gamma}{dk^2}(V^* \rightarrow HV) = \frac{G_F M_V^4}{2\sqrt{2}\pi^2} \frac{\lambda^{1/2}(M_V^2, M_H^2; k^2)}{(k^2 - M_V^2)^2} \left(1 + \frac{\lambda(M_V^2, M_H^2; k^2)}{12M_V^2/k^2} \right) . \quad (2)$$

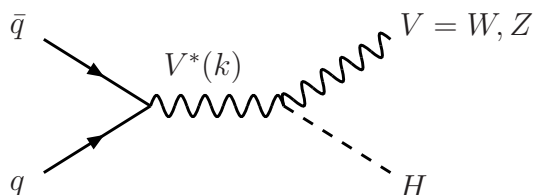


Figure 1: *Diagram for associated Higgs and vector boson production in hadronic collisions.*

The total cross section for the subprocess is obtained by integrating over k^2 :

$$\hat{\sigma}_{\text{LO}}(q\bar{q} \rightarrow VH) = \frac{G_F^2 M_V^4}{288\pi\hat{s}} (v_q^2 + a_q^2) \lambda^{1/2}(M_V^2, M_H^2; \hat{s}) \frac{\lambda(M_V^2, M_H^2; \hat{s}) + 12M_V^2/\hat{s}}{(1 - M_V^2/\hat{s})^2} , \quad (3)$$

where the reduced quark couplings to gauge bosons are given in terms of the electric charge and the weak isospin of the fermion as: $a_q = 2I_q^3, v_q = 2I_q^3 - 4Q_q s_W^2$ for $V = Z$ and $v_q = -a_q = \sqrt{2}$ for $V = W$, with $s_W^2 = 1 - c_W^2 \equiv \sin^2 \theta_W$.

The total hadronic cross section is then obtained by convoluting eq. (3) with the parton densities and summing over the contributing partons

$$\sigma_{\text{LO}}(pp \rightarrow VH) = \int_{\tau_0}^1 d\tau \sum_{q,\bar{q}} \frac{d\mathcal{L}^{q\bar{q}}}{d\tau} \hat{\sigma}_{\text{LO}}(\hat{s} = \tau s) , \quad (4)$$

where $\tau_0 = (M_V + M_H)^2/s \equiv M_{HV}^2/s$, s being the total hadronic c.m. energy, and the luminosity is defined in terms of the parton densities defined at a factorization scale μ_F .

In fact, the factorization of the $pp \rightarrow HV$ cross section in eq. (1) holds in principle at any order of perturbation theory in the strong interaction and we can thus write²

$$\frac{d\hat{\sigma}}{dk^2}(pp \rightarrow HV + X) = \sigma(pp \rightarrow V^* + X) \times \frac{d\Gamma}{dk^2}(V^* \rightarrow HV) , \quad (5)$$

where $d\Gamma/dk^2$ is given by eq. (2). Therefore, the QCD corrections to the Higgs-strahlung process, derived at NLO in Refs. [14,15], are simply the corrections to the Drell–Yan process [16,17], as pointed out in Ref. [11].

At NLO, the QCD corrections to the Drell–Yan process consist of virtual corrections with gluon exchange in the $q\bar{q}$ vertex and quark self-energy corrections, which have to be multiplied by the tree-level term, and the emission of an additional gluon, the sum of which has to be squared and added to the corrected tree-level term; see Fig. 2.

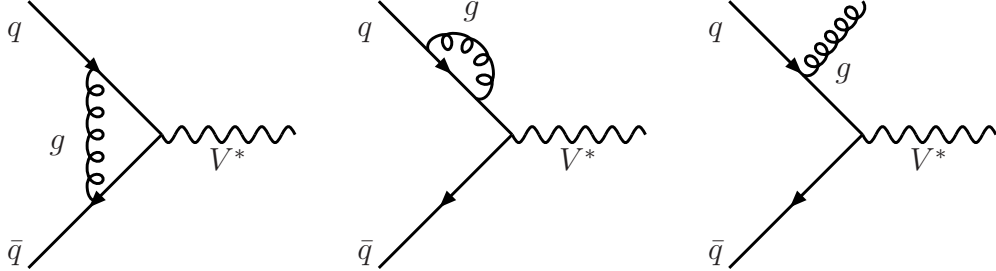


Figure 2: *NLO QCD corrections to the vector boson–quark–antiquark vertex.*

Including these contributions, and taking into account the virtuality of the vector boson, the LO cross section is modified in the following way

$$\sigma_{\text{NLO}} = \sigma_{\text{LO}} + \Delta\sigma_{q\bar{q}} + \Delta\sigma_{qg} , \quad (6)$$

with

$$\begin{aligned} \Delta\sigma_{q\bar{q}} &= \frac{\alpha_s(\mu_R)}{\pi} \int_{\tau_0}^1 d\tau \sum_q \frac{d\mathcal{L}^{q\bar{q}}}{d\tau} \int_{\tau_0/\tau}^1 dz \hat{\sigma}_{\text{LO}}(\tau zs) \omega_{q\bar{q}}(z) , \\ \Delta\sigma_{qg} &= \frac{\alpha_s(\mu_R)}{\pi} \int_{\tau_0}^1 d\tau \sum_{q,\bar{q}} \frac{d\mathcal{L}^{qg}}{d\tau} \int_{\tau_0/\tau}^1 dz \hat{\sigma}_{\text{LO}}(\tau zs) \omega_{qg}(z) , \end{aligned} \quad (7)$$

²This is only valid at first order in the electroweak coupling; at two-loop order in G_F , QCD corrections to the final state should also be taken into account. In addition, for the process $pp \rightarrow HZ$, an additional contribution will appear at $\mathcal{O}(\alpha_s^2)$ as will be discussed later.

with the coefficient functions [16]

$$\begin{aligned}\omega_{q\bar{q}}(z) &= -P_{qq}(z) \log \frac{\mu_F^2}{\tau_S} + \frac{4}{3} \left[\left(\frac{\pi^2}{3} - 4 \right) \delta(1-z) + 2(1+z^2) \left(\frac{\log(1-z)}{1-z} \right)_+ \right], \\ \omega_{qg}(z) &= -\frac{1}{2} P_{qg}(z) \log \left(\frac{\mu_F^2}{(1-z)^2 \tau_S} \right) + \frac{1}{8} [1 + 6z - 7z^2],\end{aligned}\quad (8)$$

where μ_R denotes the renormalization scale and P_{qq}, P_{qg} are the well-known Altarelli–Parisi splitting functions, which are given by [18]

$$P_{qq}(z) = \frac{4}{3} \left[\frac{1+z^2}{(1-z)_+} + \frac{3}{2} \delta(1-z) \right], \quad P_{qg}(z) = \frac{1}{2} [z^2 + (1-z)^2]. \quad (9)$$

The index $+$ denotes the usual distribution $F_+(z) = F(z) - \delta(1-z) \int_0^1 dz' F(z')$. Note that the cross section depends explicitly on $\log(\mu_F^2/Q^2)$; the factorization scale choice $\mu_F^2 = Q^2 = M_{HV}^2$ therefore avoids the occurrence of these potentially large logarithms. The renormalization scale dependence enters in the argument of α_s and is rather weak. In most of our discussion, we will set the two scales at $\mu_F = \mu_R = M_{HV}$. For this choice, the NLO corrections increase the LO cross section by approximately 30%.

3. The NNLO corrections

The NNLO corrections, i.e. the contributions at $\mathcal{O}(\alpha_s^2)$, to the Drell–Yan process $pp \rightarrow V^*$ consist of the following set of radiative corrections [see also Fig. 3a–c]:

- Two-loop corrections to $q\bar{q} \rightarrow V^*$, which have to be multiplied by the Born term.
- One-loop corrections to the processes $qg \rightarrow qV^*$ and $q\bar{q} \rightarrow gV^*$, which have to be multiplied by the tree-level qg and $q\bar{q}$ terms initiated by the diagrams shown in Fig. 2.
- Tree-level contributions from $q\bar{q}, qq, qg, gg \rightarrow V^* + 2$ partons in all possible ways; the sums of these diagrams for a given initial and final state have to be squared and added.

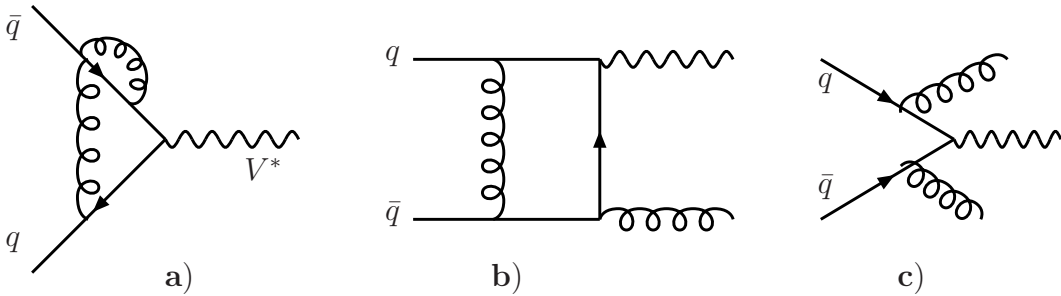


Figure 3: *Diagrams for the NNLO QCD corrections to the process $q\bar{q} \rightarrow W^*$.*

These corrections have been calculated a decade ago in Ref. [17] and recently updated [19].

However, these calculations are not sufficient to obtain a full NNLO prediction: the cross sections must be folded with the NNLO-evolved parton distribution functions (PDFs), which are necessary. The latter require the calculation of Altarelli–Parisi splitting functions up to three loops and, to this day, the latter are not completely known at this order. Nevertheless, a large number of moments of these functions are available [20]; when these are combined with additional information on the behaviour at small x , we can obtain an approximation of the splitting functions at the required order. The NNLO MRST [21] parton distributions follow this approach and can therefore be adopted for this calculation.

In the case of $pp \rightarrow HZ$ production, because the final state is electrically neutral, two additional sets of corrections need to be considered at $\mathcal{O}(\alpha_s^2)$.

Contrary to charged W bosons, the neutral Z bosons can be produced via an effective Z –gluon–gluon coupling induced by quark loops (Fig. 4). This can occur at the two-loop level in a box+triangle diagram in $q\bar{q} \rightarrow Z^*$ [which has to be multiplied by the Born term], or at the one-loop level where vertex diagrams appear for the $q\bar{q} \rightarrow gZ^*$ and $qg \rightarrow qZ^*$ processes [and which have to be multiplied by the respective $\mathcal{O}(\alpha_s)$ tree-level terms].

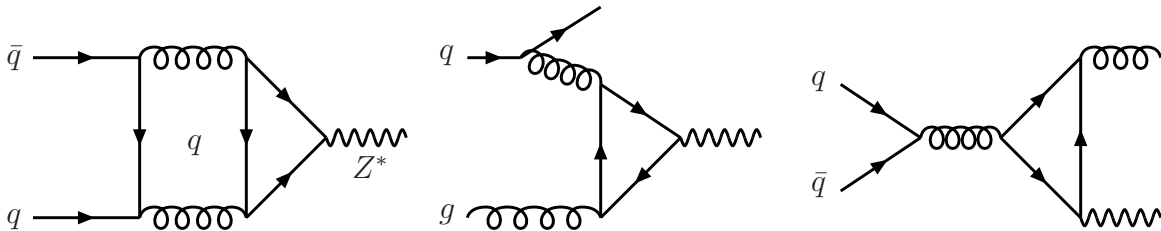


Figure 4: *Diagrams for the QCD corrections to $q\bar{q} \rightarrow Z^*$ not present in $q\bar{q} \rightarrow W^*$.*

Because gluons have only vector couplings to quarks and the effective Zgg coupling must be a colour singlet, only the axial–vector part of the $Zq\bar{q}$ coupling will contribute as a consequence of Furry’s theorem. The axial–vector of the Z coupling to quarks, $a_q = 2I_q^3$, differs only by a sign for isospin up-type and down-type quarks, so that their contribution should vanish in the case of quarks that are degenerate in mass. Thus, in the SM, only the top and bottom quarks will contribute to these topologies³.

These corrections have been evaluated in Refs. [22, 23] and have been shown to be extremely small. The one-loop corrections give relative contributions that are less than a few times 10^{-4} and thus completely negligible. The two-loop contribution is somewhat larger. However, at Tevatron energies and for partonic c.m. energies close to the Z boson mass, the contribution is still below the 1% level, and it is even smaller at the LHC [22]. These corrections can therefore be safely neglected.

³Note that additional contributions involving heavy top quarks in gluonic two-point functions are also present; however, they give zero contribution when the top quark is decoupled.

Another set of diagrams that contribute at $\mathcal{O}(\alpha_s^2)$ to ZH and not to WH production [again because of charge conservation] is the gluon–gluon-initiated mechanism $gg \rightarrow HZ$ [24, 25]. It is mediated by quark loops [see Fig. 5] which enter in two ways. There is first a triangular diagram with $gg \rightarrow Z^* \rightarrow HZ$, in which only the top and bottom quark contributions are present since, the Z boson couples only axially to the internal quarks, because of C-invariance, the contribution of a mass-degenerate quark weak-isodoublet vanishes. There are also box diagrams where both the H and Z bosons are emitted from the internal quark lines and where only the contribution involving heavy quarks which couple strongly to the Higgs boson [the top quark and, to a lesser extent, the bottom quark] are important.

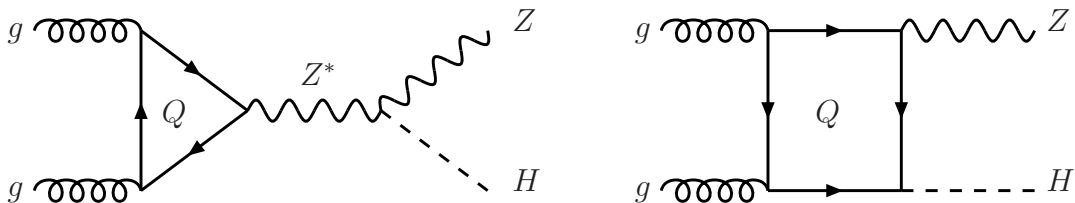


Figure 5: *Diagrams for the $gg \rightarrow HZ$ process, which contributes to $\mathcal{O}(\alpha_s^2)$.*

At the LHC, the contribution of this gluon–gluon fusion mechanism to the $pp \rightarrow HZ$ total production cross section can be substantial. This is due to the fact that the suppression of the cross section by a power $(\alpha_s/\pi)^2$ is partly compensated by the increased gluon luminosity at high-energies. In addition, the tree-level cross section for $q\bar{q} \rightarrow HZ$ drops for increasing c.m. energy and/or M_H values, since it is mediated by s -channel gauge-boson exchange.

We have recalculated the cross section for the process $gg \rightarrow HZ$ at the LHC energy $\sqrt{s} = 14$ TeV, taking into account the full top and bottom quark mass [$m_b = 5$ GeV and $m_t = 175$ GeV] dependence. The two contributing triangle and box amplitudes interfere destructively, as found in Ref. [25]. Our results agree with those given in the figures of this article, once we take the same kinematical configuration, inputs and PDFs [$\sqrt{s} = 17$ TeV and $m_t = 80, 140$ or 200 GeV]. The cross section for this process is of course negligible at the Tevatron, because of the low gluon luminosity and the reduced phase space.

4. Numerical analysis

The impact of higher order (HO) QCD corrections is usually quantified by calculating the K -factor, which is defined as the ratio of the cross sections for the process at HO (NLO or NNLO), with the value of α_s and the PDFs evaluated also at HO, over the cross section at LO, with α_s and the PDFs consistently evaluated also at LO:

$$K_{\text{HO}} = \frac{\sigma_{\text{HO}}(pp \rightarrow HV + X)}{\sigma_{\text{LO}}(pp \rightarrow HV)}. \quad (10)$$

A kind of K -factor for the LO cross section, K_{LO} , can also be defined by evaluating the latter at given factorization and renormalization scales and normalizing to the LO cross sections evaluated at the central scale, which, in our case, is given by $\mu_F = \mu_R = M_{HV}$.

The K -factors at NLO and NNLO are shown in Figs. 6 and 7 (solid black lines) for, respectively, the LHC and the Tevatron as a function of the Higgs mass for the process $pp \rightarrow HW$; they are practically the same⁴ for the process $pp \rightarrow HZ$ when the contribution of the $gg \rightarrow HZ$ component is not included. The scales have been fixed to $\mu_F = \mu_R = M_{HV}$ and the MRST sets of PDFs for each perturbative order are used in a consistent manner.

The NLO K -factor is practically constant at the LHC, increasing only from $K_{\text{NLO}} = 1.27$ for $M_H = 110$ GeV to $K_{\text{NLO}} = 1.29$ for $M_H = 300$ GeV. The NNLO contributions increase the K -factor by a mere 1% for the low M_H value and by 3.5% for the high value. At the Tevatron, the NLO K -factor is somewhat higher than at the LHC, enhancing the cross section between $K_{\text{NLO}} = 1.35$ for $M_H = 110$ GeV and $K_{\text{NLO}} = 1.3$ for $M_H = 300$ GeV with a monotonic decrease. The NNLO corrections increase the K -factor uniformly by about 10%. Thus, these NNLO corrections are more important at the Tevatron than at the LHC.

The bands around the K -factors represent the variation of the cross sections when they are evaluated at renormalization and factorization scale values that are independently varied from $\frac{1}{3}M_{HV} \leq \mu_F (\mu_R) \leq 3M_{HV}$, while the other is fixed to $\mu_R (\mu_F) = M_{HV}$; the normalization provided by the production cross section evaluated at scales $\mu_F = \mu_R = M_{HV}$. As can be seen, except from the accidental cancellation of the scale dependence of the LO cross section at the LHC, the decrease of the scale variation is strong when going from LO to NLO and then to NNLO. For $M_H = 120$ GeV, the uncertainty from the scale choice at the LHC drops from 10% at LO, to 5% at NLO, and to 2% at NNLO. At the Tevatron and for the same Higgs boson mass, the scale uncertainty drops from 20% at LO, to 7% at NLO, and to 3% at NNLO. If this variation of the cross section with the two scales is taken as an indication of the uncertainties due to the not yet calculated higher order corrections, one concludes that once the NNLO contributions are included in the prediction, the cross section for the $pp \rightarrow HV$ process is known at the rather accurate level of 2 to 3%.

Finally, we present in Fig. 7 the total production cross sections at NNLO for the processes $q\bar{q} \rightarrow HW$ and HZ at both the Tevatron and the LHC as a function of M_H . In the case of the HZ process, the contribution of the $gg \rightarrow ZH$ subprocess to the total cross section is not yet included, but it is displayed separately in the LHC case. For Higgs masses in the range $100 \text{ GeV} \lesssim M_H \lesssim 250 \text{ GeV}$, where $\sigma(q\bar{q} \rightarrow HZ)$ is significant, $\sigma(gg \rightarrow HZ)$ is at the level of 0.1 to 0.01 pb and represents about 10% of the total cross section for low M_H .

⁴Because of the slightly different phase space and scale, the K -factor for $pp \rightarrow ZH$ is not identical to the K -factor for $pp \rightarrow WH$. However, since $(M_Z^2 - M_W^2)/\hat{s}$ is small and the dependence of $d\Gamma$ in eq. (3) on k^2 is not very strong in the range that we are considering, the K -factors for the two processes are very similar.

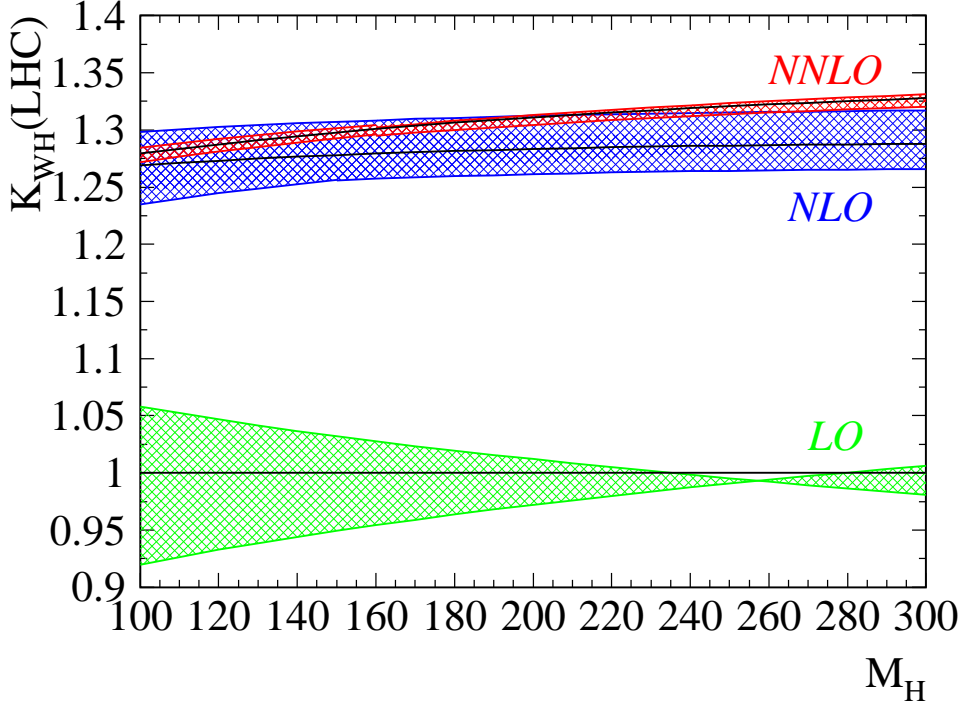


Figure 6: *The K-factors for $pp \rightarrow HW$ at the LHC as a function of M_H at LO, NLO and NNLO (solid black lines). The bands represent the spread of the cross section when the renormalization and factorization scales are varied in the range $\frac{1}{3}M_{HV} \leq \mu_R(\mu_F) \leq 3M_{HV}$, the other scale being fixed at $\mu_F(\mu_R) = M_{HV}$.*

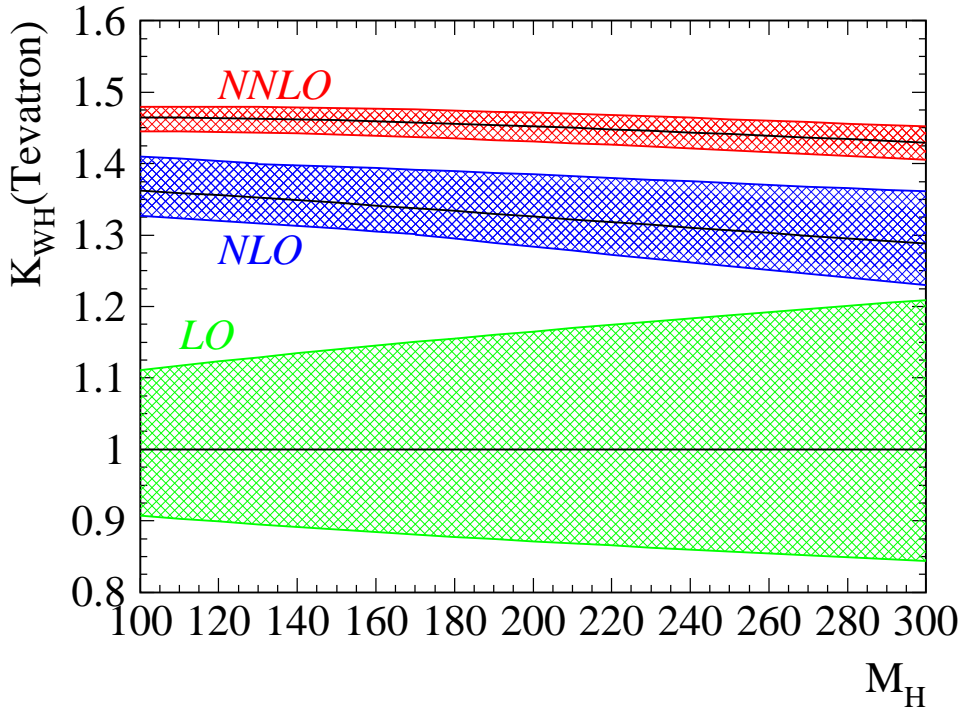


Figure 7: *The same as in Fig. 6 but for the Tevatron case, $p\bar{p} \rightarrow HW$.*

Its relative magnitude increases for higher Higgs masses; for very large M_H values, it reaches the level of the Drell–Yan cross section. However, for these large Higgs masses, the total production rate is too small to be useful in practice. Note that at the Tevatron, as expected, the cross section of the $gg \rightarrow HZ$ subprocess is very small, barely reaching the level of $\sigma(gg \rightarrow HZ) \sim 0.2$ fb for $M_H = 120$ GeV. The contribution of this subprocess can be safely neglected in this case.

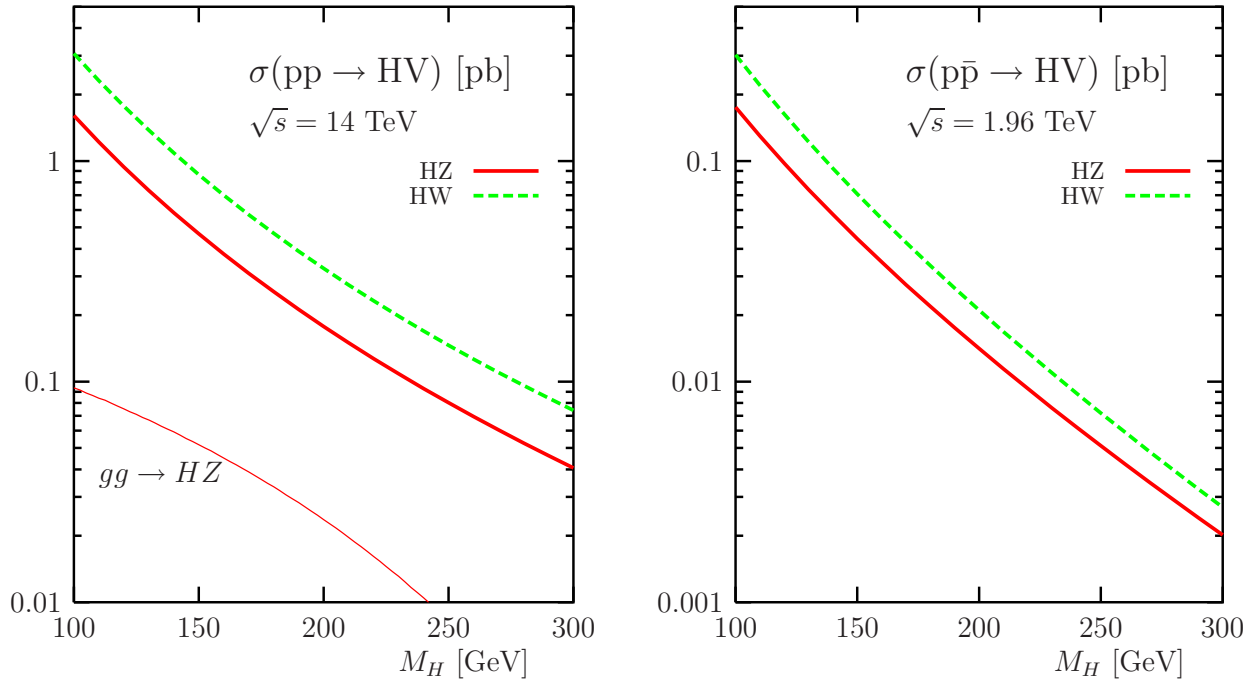


Figure 8: The total production cross sections at NNLO for $pp \rightarrow HV$ and HZ at the LHC (left) and the Tevatron (right) as a function of M_H . The MRST parton densities have been used. The contribution of the $gg \rightarrow HZ$ process is shown separately in the case of the LHC.

5. Concluding remarks

We have discussed the Higgs-strahlung processes $pp \rightarrow HV$ with $V = W, Z$ at NNLO in strong interactions. We have shown that the Drell–Yan-type corrections increase the total production cross sections by up to 3% at the LHC and by up to 10% at the Tevatron in the Higgs mass range relevant at these colliders. Because of the larger gluon luminosity at high energies, the additional contribution due to the $gg \rightarrow HZ$ subprocess can be relatively important at the LHC, and for Higgs boson masses far above 200 GeV, it becomes comparable with the $q\bar{q} \rightarrow HZ$ production cross section, but the total rate is then rather small. The scale dependence is strongly reduced from NLO, where it can reach a level close to 10%, to less than 2–3% at NNLO. These NNLO corrections are of the same order, but of opposite sign, as the $\mathcal{O}(\alpha)$ electroweak corrections to these processes, which have been calculated very recently [26].

Together with the effects of higher-order corrections, the uncertainties due to the PDFs dominate the theoretical error on the production cross section. Recently, the CTEQ [27] and MRST [28] collaborations introduced a new scheme, which gives the possibility of controlling these errors: in addition to the nominal best fit PDFs, they provided a set of $2N$ PDFs [$N = 20$ for CTEQ and 15 for MRST] at NLO [they are not yet available at NNLO], corresponding to the minima and maxima of the N eigenvectors of the matrix error of the fitting parameters. Adding the maximum and minimum deviation for each eigenvector in quadrature, we obtain an error on the total cross section at NLO of less than 5% for $M_H \lesssim 300$ (200) GeV for LHC (Tevatron) energies [29].

All these features make Higgs-strahlung one of the most theoretically clean Higgs boson production channels at hadron colliders. This will be of great importance when it comes to the determination of the properties of the Higgs boson and the measurement of its couplings. The systematic uncertainties originating from higher-order corrections and structure functions being small [a better determination of the parton distribution functions can be performed in the future], the Higgs-strahlung process will provide a clean determination of the HVV couplings times the Higgs branching ratios [the latter being measured in other Higgs production processes] if enough integrated luminosity is collected to make the statistical errors also small⁵.

This analysis can straightforwardly be extended to the case of the Minimal Supersymmetric extension of the SM [1]. The two CP-even Higgs bosons, $\Phi = h$ and H , can be produced in the same channels, $pp \rightarrow V\Phi$, and the LO cross sections are the same as the one for the SM Higgs boson, except that they are suppressed by global coupling factors, $0 \leq g_{\Phi VV}^2 \leq 1$. The standard QCD corrections are again similar to those discussed here; the additional corrections due to supersymmetric partners of quarks and gluons have to be added [note that the triangular Zgg diagrams with scalar loops give zero contribution here]. This analysis can even be extended to the case of the associated production of CP-even and CP-odd Higgs particles, $pp \rightarrow \Phi A$. Here again, the cross section can be factorized into the product of $pp \rightarrow V^*$ production and $V^* \rightarrow \Phi A$ decays, and the QCD corrections are thus the same as those discussed here. A small additional contribution originating from the one-loop subprocess $gg \rightarrow \Phi A$ [31] has to be added, though.

Acknowledgements: We thank Samir Ferrag and Michael Spira for discussions.

⁵Note that an additional systematic error of about 5% arises from the pp luminosity. To reduce all these uncertainties at the LHC, it has been suggested [30] to use the Drell–Yan processes $pp \rightarrow W, Z$ with the subsequent leptonic decays of the gauge bosons as a means of measuring directly the quark and antiquark luminosities at hadron colliders. The errors on the cross sections for all processes dominated by $q\bar{q}$ scattering, such as the Higgs-strahlung discussed here, when normalized to the Drell–Yan rate, would lead to a total systematical uncertainty of less than 1%. In this case, the dominant part of the K -factor for Higgs-strahlung will drop out in the ratio.

References

- [1] For a review of the Higgs sector, see : J.F. Gunion, H.E. Haber, G.L. Kane and S. Dawson, “The Higgs Hunter’s Guide”, Addison–Wesley, Reading 1990.
- [2] The LEP and SLC Electroweak Working Groups, hep-ex/0112021.
- [3] M. Carena et al., Report of the Higgs Working Group for “RUN II at the Tevatron”, hep-ph/0010338.
- [4] Proceedings of the Les Houches Workshops on “Physics at TeV Colliders”, A. Djouadi et al., hep-ph/0002258 (1999) and D. Cavalli et al., hep-ph/0203056 (2001).
- [5] CMS Collaboration, Technical Proposal, CERN/LHCC/94-38 (1994); ATLAS Collaboration, Technical Design Report CERN/LHCC/99-15 (1999);
- [6] S. Glashow, D. Nanopoulos and A. Yildiz, Phys. Rev. D18 (1978) 1724; E. Eichten, I. Hinchliffe, K. Lane and C. Quigg, Rev. Mod. Phys. 56 (1984) 579.
- [7] A. Stange, W.J. Marciano and S. Willenbrock, Phys. Rev. D49 (1994) 1354 and D50 (1994) 4491.
- [8] H. Georgi et al., Phys. Rev. Lett. 40 (1978) 692; A. Djouadi, M. Spira and P.M. Zerwas, Phys. Lett. B264 (1991) 440; S. Dawson, Nucl. Phys. B359 (1991) 283; M. Spira et al., Phys. Lett. B318 (1993) 347 and Nucl. Phys. B453 (1995) 17.
- [9] R. Harlander and W. Kilgore, Phys. Rev. Lett. 88 (2002) 201801; C. Anastasiou and K. Melnikov, Nucl. Phys. B646 (2002) 220; V. Ravindran, J. Smith and W. L. van Neerven, hep-ph/0302135; S. Catani, D. de Florian, M. Grazzini and P. Nason, hep-ph/0306211.
- [10] J. Gunion, Phys. Lett. B253 (1991) 269; Z. Kunszt, Z. Trocsanyi and J. Stirling, Phys. Lett. B271 (1991) 247.
- [11] R. Kleiss, Z. Kunszt and W.J. Stirling, Phys. Lett. B253 (1991) 269; J.F. Gunion, G. Kane et al., published in Snowmass Summer Study 1990, pp. 0059-81.
- [12] D. Zeppenfeld, R. Kinnunen, A. Nikitenko and E. Richter-Was, Phys. Rev. D62 (2000) 013009.
- [13] R. Harlander and W. Kilgore, Phys. Rev. D68 (2003) 013001.
- [14] T. Han and S. Willenbrock, Phys. Lett. B273 (1990) 167.

- [15] H. Baer, B. Bailey and J. Owens, Phys. Rev. D47 (1993) 2730; J. Ohnemus and W. Stirling, Phys. Rev. D47 (1993) 2722; S. Mrenna and C.P. Yuan, Phys. Lett. B416 (1998) 200; M. Spira, Fortschr. Phys. 46 (1998) 203; A. Djouadi and M. Spira, Phys. Rev. D62 (2000) 014004.
- [16] G. Altarelli, R.K. Ellis and G. Martinelli, Nuc. Phys. B157 (1979) 461; J. Kubar-André and F. Paige, Phys. Rev. D19 (1979) 221.
- [17] R. Hamberg, W.L. van Neerven and T. Matsuura, Nucl. Phys. B359 (1991) 343; (E) ibid. B644 (2002) 403.
- [18] G. Altarelli and G. Parisi, Nucl. Phys. B126 (1977) 298.
- [19] R.V. Harlander and W.B. Kilgore, as in Ref. [9].
- [20] S.A. Larin, T. van Ritbergen and J.A.M. Vermaseren, Nucl. Phys. B427 (1994) 41 and B492 (1997) 338; A. Rétey and J.A.M. Vermaseren, Nucl. Phys. B604 (2001) 281.
- [21] A.D. Martin, R.G. Roberts, W.J. Stirling and R.S. Thorne, Phys. Lett. B531 (2002) 216.
- [22] D.A. Dicus and S.S.D. Willenbrock, Phys. Rev. D34 (1986) 148.
- [23] K. Hikasa, Phys. Rev. D29 (1984) 1939; R. Gonsalves, C. Hung and J. Pawlowski, Phys. Rev. D46 (1992) 4930; P. Rijken and W. van Neerven, Phys. Rev. D52 (1995) 149.
- [24] V. Barger et al., Phys. Rev. Lett. 57 (1986) 1672; D. Dicus and C. Kao, Phys. Rev. D38 (1988) 1008; (E) ibid. D42 (1990) 2412.
- [25] B. Kniehl, Phys. Rev. D42 (1990) 2253.
- [26] M.L. Ciccolini, S. Dittmaier and M. Krämer, hep-ph/0306234.
- [27] The CTEQ Collaboration, J. Pumplin, D.R. Stump, J. Huston, H.L. Lai, P. Nadolsky and W.K. Tung, JHEP 0207 (2002) 012, hep-ph/0201195.
- [28] The MRST Collaboration, A.D. Martin, R.G. Roberts, W.J. Stirling and R.S. Thorne, Eur. Phys. J.C28 (2003) 455, hep-ph/0211080.
- [29] S. Ferrag and B. Laforge, Note ATL-COM-PHYS-2003-13; A. Djouadi and S. Ferrag, contribution to the Les Houches Workshop 2003, to appear. See also Ref. [26].
- [30] M. Dittmar, F. Pauss and D. Zürcher, Phys. Rev. D56 (1997) 7284.
- [31] T. Plehn, M. Spira and P.M. Zerwas, Nucl. Phys. B479 (1996) 46; A. Djouadi, W. Kilian, M. Mühlleitner and P.M. Zerwas, Eur. Phys. J. C10 (1999) 45.